RESPONSE TO PHOTIC STIMULATION AS A MEASURE OF CORTICAL EXCITABILITY IN EPILEPSY PATIENTS

A PREPRINT

Michaela J. Vranic-Peters
Department of Biomedical Engineering
The University of Melbourne

Patrick O'brien
Department of Medicine
St Vincent's Hospital Melbourne
The University of Melbourne

Udaya Seneviratne
Department of Clinical Sciences
Monash University

Ashley Reynolds
Department of Biomedical Engineering
The University of Melbourne

Alan Lai
Department of Medicine
The University of Melbourne

David Grayden
Department of Biomedical Engineering
The University of Melbourne

Mark Cook
Department of Medicine
St Vincent's Hospital Melbourne
The University of Melbourne

Andre Peterson
Department of Medicine
St Vincent's Hospital Melbourne
The University of Melbourne

April 23, 2023

ABSTRACT

Studying states and state transitions in the brain is challenging due to the nonlinear, complex dynamics present. In this research, we analyse the brain's response to non-invasive perturbations. Perturbation techniques offer a powerful method for studying complex dynamics [1], though their translation to human brain data is under-explored. This method involves applying small inputs, in this case via photic stimulation, to a system and measuring its response. Sensitivity to perturbations can forewarn a state transition [1], therefore biomarkers of the brain's perturbation response or 'cortical excitability' could be used to indicate seizure transitions [2; 3; 4]. However, perturbing the brain often involves invasive intracranial surgeries [5] or expensive equipment as in transcranial magnetic stimulation (TMS) which is only accessible to a minority of patient groups [6; 7], or animal model studies [8]. Photic stimulation is a widely used diagnostic technique in epilepsy [9] that can be used as a non-invasive perturbation paradigm to probe brain dynamics during routine electroencephalography (EEG) studies in humans. This involves changing the frequency of strobing light, sometimes triggering a photo-paroxysmal response (PPR), which is an electrographic event that can be studied as a state transition to a seizure state. We investigate alterations in the response to these perturbations in patients with genetic generalised epilepsy (GGE), with (n=10) and without (n=10) PPR, and patients with psychogenic non-epileptic seizures (PNES; n=10), compared to resting controls (n=10). Metrics of EEG time-series data were evaluated as biomarkers of the perturbation response including variance, autocorrelation, and phase-based synchrony measures. We observed considerable differences in all group biomarker distributions during stimulation compared to controls. In particular, variance and autocorrelation demonstrated greater changes in epochs close to PPR transitions compared to earlier stimulation epochs. Comparison of PPR and spontaneous seizure morphology found them indistinguishable, suggesting PPR is a valid proxy for seizure dynamics. Also, as expected, posterior channels demonstrated the greatest change in synchrony measures, possibly reflecting underlying PPR pathophysiology mechanisms [9]. We clearly demonstrate observable changes at a group level in cortical excitability in epilepsy patients as a response to perturbation in EEG data. Our work re-frames photic stimulation as a non-invasive perturbation paradigm capable of inducing measurable changes to brain dynamics.

1 Introduction

Understanding brain function is challenging due to the nonlinear, complex dynamics present. Methods from statistical physics relating to dynamical systems theory have been applied to various research domains studying other complex, nonlinear systems, including ecological population changes [10] weather [11], and economics [12]. Researchers have begun to study the brain using these techniques, including the study of brain state transitions in epilepsy patients [13; 14; 15; 2].

Epilepsy is a brain disease characterized by abnormal electrical brain activity and unprovoked recurrent seizures (spiking activity visible on an EEG with clinical manifestations), that occurs in approximately 1% of the population [16]. These are generally detected on electroencephalography (EEG) and other brain recording techniques, and the transition to seizure can be conceptualised as a critical transition [13; 17; 18]. Metrics that identify changes in system dynamics before these transitions called 'early warning signs', have been observed in the EEG of epilepsy patients before seizures [3; 2]. These include increased variance, autocorrelation, and sensitivity to perturbation (a small external input).

As a system approaches a state transition, it becomes less resilient to change and more sensitive to perturbations, such that it is slower to return to equilibrium [1]. This phenomenon is often characterised as 'critical slowing'. Since increased sensitivity to perturbation can forewarn a state transition, biomarkers of the brain's perturbation response or 'cortical excitability' [19] could be used to track brain dynamics towards transitions to different states, including seizure states or other altered states of consciousness. Measures of the perturbation response differ from previous critical slowing literature which employs measures in a passive manner to indicate underlying dynamics, rather than actively inducing and measuring a response. In this way, perturbation methods have the potential to offer unique experimental insights, and the inputs can be well-controlled, and stimulation can be easily time-stamped. However, delivering perturbations to the brain can prove imprecise and invasive in practice, such that studies of perturbation are often *in-silico*, *in-vitro*, or use animal models, rather than human brains.

Animal studies have indicated that active measures of EEG recordings track cortical excitability in mice [8] add Wei's study if published soon. Perturbing the brain in living humans often involves invasive intracranial surgeries [5; 20; 21; 22; 23], or expensive equipment only accessible to a minority of patient groups such as transcranial magnetic stimulation (TMS), though the perturbation is diffuse and spatially non-specific [6; 7; 24]. In these contexts, epilepsy is commonly studied, where the response to electrical stimulation is used to indicate seizure susceptibility. However, they rely on the eventual observations of seizures to infer their predictive power. This is problematic as seizure rarity necessitates long-term recordings which are time-consuming to record and parse.

Photic stimulation is a widely used diagnostic technique [9], that could be used as a non-invasive perturbation paradigm to probe brain dynamics during routine EEG studies in humans. It involves changing the frequency of strobing light, sometimes triggering a photo-paroxysmal response (PPR), which is an electroencephalographic event visible on EEG. Generally, it's primary clinical relevance is to diagnose photosensitive epilepsy, though we argue that it offers a safe, accessible research method for brain perturbation studies. There is also precedence for using photic stimulation as a research paradigm. Previous work investigating anti-seizure medication (ASM) in photosensitive epilepsy patients, used the suppression or reduction of PPR during photic stimulation to indicate ASM effectiveness [25; 26; 27; 28; 29]. These studies highlight the neuromodulatory effect of ASMs on cortical excitability, and the potential use of photic stimulation in evaluating drug efficacy, though they rely on binary evaluations of PPR presence and photosensitivity. We aim to extend this paradigm to develop biomarkers sensitive to changes of cortical excitability, that do not necessarily require PPR presence, making them generalisable to other types of epilepsy. In fact, many non-epileptic patients demonstrate abnormal excitability in response to photic stimulation, including migraine [30; 31], parkinson's disease, head trauma and alcohol withdrawal [32], making biomarkers of cortical excitability in response to photic stimulation potentially applicable for evaluating state transitions related to other diseases of altered brain function.

Prior research has demonstrated that photosensitive individuals show elevated responses of cortical excitability to photic stimulation. A measure of phase clustering called relative phase clustering index (rPCI) was used to compare photic stimulation trials where PPR was or was not elicited [15]. They found that with no PPR, the highest rPCI was that of the driving frequency of stimulation, but when stimulation induced PPR, that particular frequency and it's harmonics were the dominant rPCI . An extended study used rPCI to indicate greater probability of epileptic seizures [5]. In a different study, visually evoked potential (VEP) amplitudes were used to indicate the response to photic stimulation, and found higher amplitudes in photosensitive individuals compared to controls, especially in occipital areas [33]. In fact, in photosensitive individuals, TMS over the visual cortex induced a stronger suppression of visual perception and had lower phosphene thresholds compared to healthy controls, suggesting increased excitability of the visual cortex may underlie PPR pathophysiology. Studies have used other measures related to the power spectrum to indicate changes in excitability. For instance, reduced inhibition of alpha rhythm generating networks was associated with photosensitive

epilepsy [34], and stimulation via flashed chromatic gratings induced alpha desynchronisation in posterior electrodes [35].

Related to this measure, are changes in the power spectrum, which can be related to the autocorrelation function via the Wiener-Khinchin theorem [**?**]. For example, we may expect increased dominance in lower frequencies during critical slowing down, which also relates to the increased autocorrelation measures and increased long-range temporal associations, as demonstrated in the seizure prediction study previously mentioned [36]. Increased spatial similarity can also be observed as an EWS, via a multitude of synchrony measures. This is supported by findings of increased phase synchronisation in the gamma frequency range in EEG, being associated with increased neuronal excitability in epilepsy patients [3]. Another study used changes in power spectral density (PSD) from low frequency bands to predict seizures from EEG recordings [36].

To evaluate changes to brain dynamics as a result of photic stimulation, we will compare distributions of cortical excitability biomarkers between groups of individuals with epilepsy and resting healthy controls. This work can be motivated theoretically from observations of stochastic descriptions of dynamical systems. In such descriptions, the temporal structure can be described in terms of statistical distributions which change as a transition is approached [37; 38]. While it is not conceivable to capture brain dynamics analytically, latent distributions were inferred from data in models of neural dynamics underlying transitions in the brain. In fact, we believe the comparison of distributions of statistical moments of timeseries measures offers a data-driven method for inferring changes to system dynamics.

Markers of critical transitions have previously only been observed in focal epilepsy patients, and we aim to observe them during this generalised PPR response. Also, unlike previous studies, we aim to compare different epileptic populations in order to compare how photic stimulation effects these different groups, including patients with genetic generalised epilepsy (GGE) who are photosensitive, GGE patients who are not photosensitive, as well as patients with Psychogenic Non-Epileptic Seizures (PNES), compared to healthy controls.

We expect to observe early warning signs of a PPR transition that are identifiable via changes of a particular metric's distribution over time. These include changes in variance and autocorrelation function widths of brain activity, as well as in phase-based synchrony measures, . In particular, we expect the greatest increases to be demonstrated in the photosensitive GGE (PPR) group, just prior to a PPR, where they likely experience heightened cortical excitability.

2 Methods

2.1 Participants

The study was conducted using data obtained retrospectively from databases of Department of Neurosciences, St. Vincent's Hospital, Melbourne, over the period of May 2012 - August 2022. This included contemporaneous EEG and ECG recordings with photic stimulation from 10 patients with genetic generalised epilepsy (GGE) and photoparoxysmal response (PPR), 10 GGE patients without PPR, and 10 patients with psychogenic non-epileptic seizures (PNES). Diagnosis of GGE was established using International League Against Epilepsy (ILAE) criteria [39]. The diagnosis of PNES was confirmed with the consensus of at least two epilepsy specialists following video-EEG monitoring using criteria from a previous study [40]. Clinical data for all patients is summarised in table 1, with a patient-specific breakdown in Table S1.

Table 1: Summary of clinical data for participants in all groups.

	GGE with PPR	**GGE without PPR**	**PNES**
*Age**	13-28 (*M=18.4*, *SD=4.54*)	17-41 (*M=24.3*, *SD=8.59*)	16-58 (M=35.3, SD=13.27)
Gender	5F, 5M	8F, 2M	4F, 6M
*Syndrome***	3 JAE 3 JME 1 CAE 2 GTCSO 1 GGE unspecified	3 JAE 3 JME 1 CAE 3 GTCSO	10 PNES
*Seizure types****	2 Absence 1 Myoclonic 2 GTCS 3 GTCS + Absence 2 GTCS + Myoclonic	1 Absence 3 GTCS 3 GTCS + Absence 2 GTCS + Myoclonic 1 GTCS + Myoclonic + Absence	Non-Epileptic

*ASMs*****	1 LEV 2 VPA 3 LTG + VPA 4 None	2 VPA 4 LTG + VPA 1 LTG + Topiramate 1 LTG + VPA + Piracetam 2 None	10 None

*Age at time of recording.
**Juvenile Absence Epilepsy (JAE), Juvenile Myoclonic Epilepsy (JME), Childhood Absence Epilepsy (CAE), Generalised Tonic-Clonic Seizures Only (GTCSO), Psychogenic Non-epileptic Seizures (PNES).
***Generalised Tonic-Clonic Seizure (GTCS). ****Anti-seizure Medication (ASM); Lamotrigine (LTG); Valproate (VPA); Levetiracetam (LEV).

2.1.1 Healthy Controls

Healthy control EEG data was obtained from an open source repository, originally described and analysed in a study by Torkamani-Azar and colleagues [41]. Control data included ten healthy adults aged 22-45 ($M = 30.25$, $SD = 6.95$), 6 were female and 4 were male. For each control subject, we analysed 2.5 minutes of eyes-closed, resting-state EEG. The eyes-closed condition was chosen for consistency, since our analysis focuses on stimulation epochs in which participants were instructed to close their eyes. More information regarding recording method is provided in the original study. Electrodes were selected to match our data, and sampling rate was conserved. The same EEG pre-processing and measure calculations were used for this control dataset.

2.2 Electroencephalography recording

Electroencephalography (EEG) data were acquired with Compumedics digital EEG system (Compumedics Ltd, Melbourne, Australia). Scalp electrodes were placed according to the 10-20 international system. All EEGs were recorded with a bandwidth of 0.5 to 70Hz at a sampling rate of 256Hz according to a standard protocol [32] including provocation techniques such as hyperventilation and intermittent photic stimulation (IPS) (as illustrated in figure 1). Photo-paroxysmal response (PPR) was identified through visual inspection of the recordings, defined as epileptiform discharges triggered by IPS visible on the EEG. For a number of participants, EEG recordings were extended throughout the day. In four participants, spontaneous seizures were observed hours after photic stimmulation.

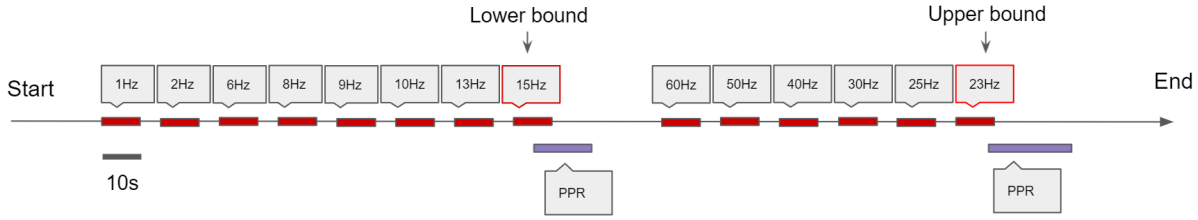

Figure 1: During the procedure, a technician increases the frequency of each subsequent photic stimulation until a Photo-Paroxysmal Response (PPR) is triggered, and the lower bound is found. Then, the technician starts from a high frequency and decreases the frequency of subsequent stimulations until another PPR is triggered, and an upper bound is found. These lower and upper bounds are indicative of the range of frequencies that trigger a PPR response specific to that patient.

For GGE (PPR) participants, the ordering of stimulation frequencies often differed after their first PPR was observed; stimulation frequencies were sometimes repeated in an attempt to elicit PPR again, and sometimes alternated to high frequencies to determine an upper sensitivity range, as is convention. It is not clear whether stimulation order effects exist, whether or not this depends on frequency, and whether refractory effects may exist after PPR that effects propensity for further PPR. Therefore, in an attempt to control for these confounding variables, we only analysed data before the first PPR. For GGE (no PPR) and PNES participants, stimulation frequency ordering was the same. In order to account for confounding effects of frequency-dependent responses, We only included stimulation epochs up to 15Hz in GGE (no PPR) and PNES groups in our analyses, as we observed PPR at or before 15Hz in all GGE (PPR) participants.

2.3 Pre-processing

Analysis was performed by importing raw data files from Profusion EEG 5 into MATLAB R2021a. Pre-processing was kept intentionally minimal in order to conserve meaningful signal. To remove DC drift and allow comparison of various measures, channel-wise moving average was subtracted from the signal, with a window of 2 seconds (512 samples). This was also used for ECG signal, after which no further processing was performed.

For variance and autocorrelation measures, we applied bandpass filters between 0.1 and 70Hz to reduce high frequency artifact. For phase-based measures, this filtering step was ommitted, as more narrow bandpass filtering is later applied to calculate the measure.

To normalize the data, we focused on making the majority of the signal comparable between different channels with varying ranges, allowing tail values but without being overly skewed by the presence of artefacts distorting the re-normalised range. Therefore, we applied z-score normalisation using the native MATLAB `normalize` function, using the `medianiqr` argument to centre the data at 0 and ensure an interquartile range of 1, with a window length of two seconds. In GGE (PPR) participants, since only data before their first PPR was analysed, normalization was not affected by the high amplitude spiking during PPR.

2.4 Measures

To capture the hypothesised rapid dynamics, measures generally used small windows with maximal overlap, and are described in detail below.

2.4.1 Variance and autocorrelation

Variance and autocorrelation were calculated for each non-reference EEG channel (*n=19*), and a single ECG channel.

The variance of the signal was calculated for each channel with a moving window of two seconds (512 samples), with overlapping steps of one sample using the native MATLAB `movvar` function. A measure of the autocorrelation function called the autocorrelation function width (ACFW). Using the same aforementioned window and overlap, the autocorrelation function was first calculated using MATLAB's `xcorr` function, and the width in samples was measured at the half prominence of the function peak, centered at it's maximum (always with a lag of 1).

2.4.2 Phase-based synchrony measures

To calculate phase-based synchrony measures, we obtain the phase-angle time series $\phi(t)$ (the instantaneous phase of each sample in the time-series) by constructing an analytic signal where the real component is the original time-series $x(t)$, and the complex component is the Hilbert transform of the real signal $\mathfrak{H}[x(t)]$. In other words, the analytic signal is the product of the envelope and instantaneous phase of the original timeseries:

$$x_{\text{analytic}}(t) = x(t) + i\mathfrak{H}[x(t)] = A(t)e^{i\phi(t)} \tag{1}$$

Note that this only holds if the original signal satisfies Bedrosian's Product Thoerem, which requires that the signal is narrow-banded using a band-pass filter [42]. To do this, we filtered the normalised data using an elliptic filter, which is a zero-phase filter that circumvents phase shifting [43]. Specifically, a filter was constructed using MATLAB's `designfilt` function, using the `bandpassiir` filter, with a filter order of 10, pass-band frequency limits according to the upper and lower limits of standard EEG frequency bands (delta: 1.5-4 Hz; theta: 4-8 Hz; alpha: 8-12 Hz; beta: 13-30 Hz; gamma: 30-70 Hz), a pass-band ripple of 3, and stop-band attenuation of 40.

Relative phase
Cosine of the Relative Phase (CRP: [44]) is calculated by taking the cosine of the instantaneous phase difference between two channels: $cos(\Delta\phi(t))$, where $\phi_x(t) - \phi_y(t)$ obtained from the original channel timeseries $x(t)$ and $y(t)$ with the method previously explained for a given frequency band. This produces a measure ranging from -1 to 1, where magnitudes close to 1 denote high synchrony. Values close to -1 also arguably demonstrate a highly synchronous event, since this is produced when there is a phase difference of exactly π, known as an anti-phase relationship [44]. Measures were considered for each combination of non-reference channels ($n = 19$), resulting in $n(n-1)/2 = 171$ unique combinations of channels.

Magnitude of the average phase vector
We also calculated the average synchrony between sets of channels using the average phase vector for a given sample.

For N oscillators, with instantaneous phases θ_j for $j = 1, 2, ...N$, their position can be represented on the unit circle by $e^{i\theta_j}$. Then, the complex number z is the average of their positions:

$$z = \frac{1}{N} \sum_{j=1}^{N} e^{i\theta_j} \tag{2}$$

We find the magnitude of z using MATLAB's native `abs` function. This produces a value from 0 to 1, where 0 represents no synchrony, or a uniform distribution, and 1 if all phases were equal over all channels for a given time sample. See figure 2 for an example. We calculated the magnitude of the average phase vector over all 19 channels and designate this *global synchrony*, as well as over 6 posterior channels only (P3, P4, T5, T6, O1, O2) and designate this *posterior synchrony*.

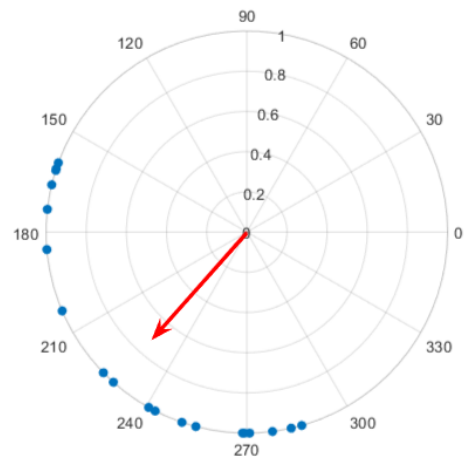

Figure 2: Each of 19 channels are shown on the unit circle as a blue dot, representing the instantaneous phase for a given time sample. The average phase is indicated by the direction of the red vector on the unit circle, and it's length corresponds to their similarity, where a perfect alignment of phase would produce a length of 1, and a uniform distribution around the circle would be 0.

The magnitude of the mean phase vector can also be calculated over an epoch of time. For N oscillators over an epoch containing S samples, the instantaneous phases $\theta_{j,k}$ for channels $j = 1, 2, ...N$ and time samples $k = 1, 2, ...S$, can be represented on the unit circle by $e^{i\theta_{j,k}}$. Then, the complex number $\hat{z}$ is the average of their positions:

$$\hat{z} = \frac{1}{N} \frac{1}{S} \sum_{k=1}^{S} \sum_{j=1}^{N} e^{i\theta_{j,k}} \tag{3}$$

Again, the magnitude of this vector produces a value from 0 to 1, where 0 represents no synchrony, or a uniform distribution, and 1 if all phases were equal between all channels over all time samples in the epoch. We designate this measure *time-varying synchrony*.

2.5 Analysis strategies and statistics

2.5.1 Clinical characteristics

Differences in ages between the four groups were evaluated using a one-way ANOVA (using the `anova1` function from the MATLAB Statistics and Machine Learning Toolbox: SML). If significance was observed, follow-up multiple comparisons were evaluated using Tukey's honestly significant difference (HSD) procedure (by passing the `stats` struct returned from the ANOVA into `multcompare` from the SML Toolbox).

Categorical clinical characteristics like sex were examined between all four groups using Pearson's chi-squared test of independence (using the `crosstab` function from SML). Differences in ASM, syndrome, and seizure type(s) were also evaluated using this test, between the two GGE groups (with and without PPR) only, since PNES participants were

not taking ASMs and were currently exhibiting non-epileptic seizures. Categories of ASM and seizure type(s) were considered distinct for each unique combination, as grouped in table 1, since this allows for distinction of combinations that may be clinically significant.

The aforementioned tests were deemed significant with a *p*-value less than 0.05. Note that Tukey's HSD procedure adjusts p-values for pair-wise multiple comparisons automatically.

2.5.2 The photo-paroxysmal response

We compared time-frequency spectrograms of PPR events and spontaneous seizures for the four participants (P1, P2, P5, P6) for which both events were available. To generate the spectra, unfiltered epochs were fed to MATLAB's `spectrogram` with window size of 256 samples, overlap of 128, and transform (nfft) length of 512 samples. Other PPR characteristics including PPR count, duration, and lower and upper frequency bounds are also measured for each participant.

2.5.3 Measures

To investigate the hypothesis that photic stimulation perturbs brain dynamics towards a more excitable state, that is measurable via changes to timeseries measures, we compare distributions of a number of measures during photic stimulation epochs, compared to a control distribution. Substantial deviations from the control distribution suggests a shift in dynamics of the underlying system.

Photic stimulation distributions contain epochs before the first PPR in the GGE (PPR) group, or before the 15Hz stimulation in the GGE (no PPR) and PNES groups. We also examine an additional pre-PPR epoch distribution in the GGE (PPR) group only, containing the closest full stimulation epoch before (ie not overlapping) the first PPR event. We hypothesise that this pre-PPR distribution may demonstrate greater changes to the measures, indicating heightened cortical excitability - compared to earlier epochs.

Since sufficient quality resting state data from the photic stimulation recordings was not available, we compare our data to distributions of healthy controls during eyes-closed, resting EEG. To create the control distributions, we randomly sampled 10s epochs from the full measure timeseries, with equal representation from the individuals of the cohort. This constructed distribution emulated the process of pooling 10s stimulation epochs in the epileptic cohort groups.

We also investigated whether measures of synchrony would change with photic stimulation. The relative phase measure contained significant degrees of freedom (unique channel pairs = 171, frequency bands = 5, resulting in 855 potential comparisons), so we investigated whether factor analysis could reduce the parameter space by identifying channels that demonstrated the greatest variation. Factor analyses of the GGE (PPR) stimulation epochs (using `factoran` from SML, with 5 factors to generate the maximum likelihood estimate) were carried out for each frequency band separately to investigate whether variation was also frequency-band dependent.

To further investigate whether measures varied by channel, and whether this is apparent in posterior channels reflecting underlying posterior pathophysiology, we compared posterior and global synchrony distributions to the corresponding control distributions. Differences were evaluated using two-factor Kolmogorov-Smirnov tests, with group as one factor and frequency band as the other. This test evaluates the difference between empirical cumulative distribution functions (CDF), using rank-based comparisons. This is appropriate considering variance, autocorrelation function width, and synchrony measures demonstrated non-parametric distributions through inspection of q-q plots. The Kolmogorov-Smirnov test identifies small differences in large datasets as significant even when differences seem trivial [45], therefore we randomly sampled from the group distributions to create datasets with 500 samples, in accordance with sample size recommendations (CITE). Bonferroni correction, considered the most conservative multiple-comparison correction, was carried out (the standard *p*-value was divided by 40: 5 frequency bands x 4 distributions x 2 sets of channels), requiring a *p*-value less than 0.00125 for significance.

3 Results

3.1 Participant clinical characteristics

One-way ANOVA identified a difference in age between at least two groups ($F(3, 36) = 6.77, p < 0.001$). Post-hoc analyses revealed that the following significant differences existed: the GGE (PPR) group had lower ages compared to the PNES group ($p < 0.001$, 95% $C.I. = [-27.77, -6.03]$) and compared to controls ($p = 0.018$, 95% $C.I. = [-23.42, -1.68]$). The GGE (no PPR) group also had lower ages compared to the PNES group ($p < 0.046$, 95% $C.I. = [-21.87, -0.13]$). We did not reject the null hypothesis that group and sex are independent ($\chi^2(3) = 3.58, p = 0.31$), therefore groups did not differ in gender ratio.

We also investigated whether ASM, syndrome, and seizure type differed between the two GGE (with and without PPR) groups. We did not reject the null hypothesis of independence between group and ASM ($\chi^2(5) = 3.81, p = 0.58$), syndrome ($\chi^2(4) = 3.53, p = 0.47$), or seizure type ($\chi^2(5) = 1.87, p = 0.87$), therefore these groups did not differ in the spread in these variables (see table 1 for a breakdown of categories).

3.2 The photo-paroxysmal response (PPR)

As can be seen in Table 2, GGE patients with PPR exhibit individualised responses to photic stimulation, including differences in their photosensitivity ranges as well as PPR length.

Table 2: Participant-specific information about PPR events

Participant	**Lower and upper frequency (Hz) bounds**	**PPR count (n)**	**Average PPR length (s)**
1	15-23	2	22.69
2	15-20	2	2.93
3	15-23	2	1.58
4	18-30	2	0.81
5	8-30	2	4.00
6	8-25	2	2.25
7	13	1	1.47
8	9-30	5	3.26
9	13-50	3	2.15
10	13-25	5	1.55

We compared the transition to PPR events spontaneous seizures by their time-varying frequency spectra by visual inspection (Fig. 3). Though spectra varied according to the individual, we observed changes to the distributions of power per frequency bin at the transition, including increased power especially in delta and theta frequencies. The spectral dynamics of PPR and seizure transitions appear similar.

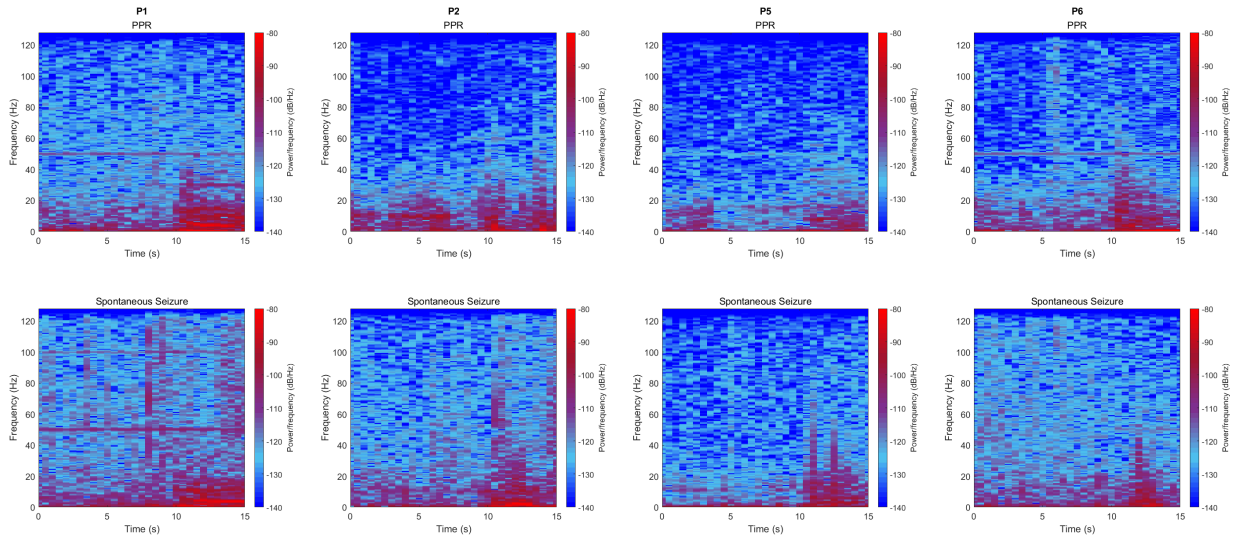

Figure 3: Time-varying frequency spectra for PPR (top row) and spontaneous seizure (bottom row) transitions which occur at the 10s mark in each subplot. Columns are different participants, and data is sourced from the 'O2' channel (similar spectra were observed in other channels). Time in seconds is shown on the x-axis, frequencies up to 128Hz are shown on the y-axis, and power per frequency bin for a given window of samples is represented as a colour, where values correspond to a colormap (see legend), where higher values are bright red, and lowest values are deep blue. In general, increased power can be observed from the 10s PPR/seizure transition point, especially in lower frequencies. Note that vertical lines at 50Hz is a power line artifact.

3.3 Measures

We examined whether measures could track individualised responses to perturbations by examining the timeseries of measures from GGE (PPR) participants as a PPR approaches.

3.3.1 Variance and autocorrelation

In general, we observed an increase in variance during stimulation epochs close to a PPR (see Fig. 4 and Supp. Fig. S1 for examples).

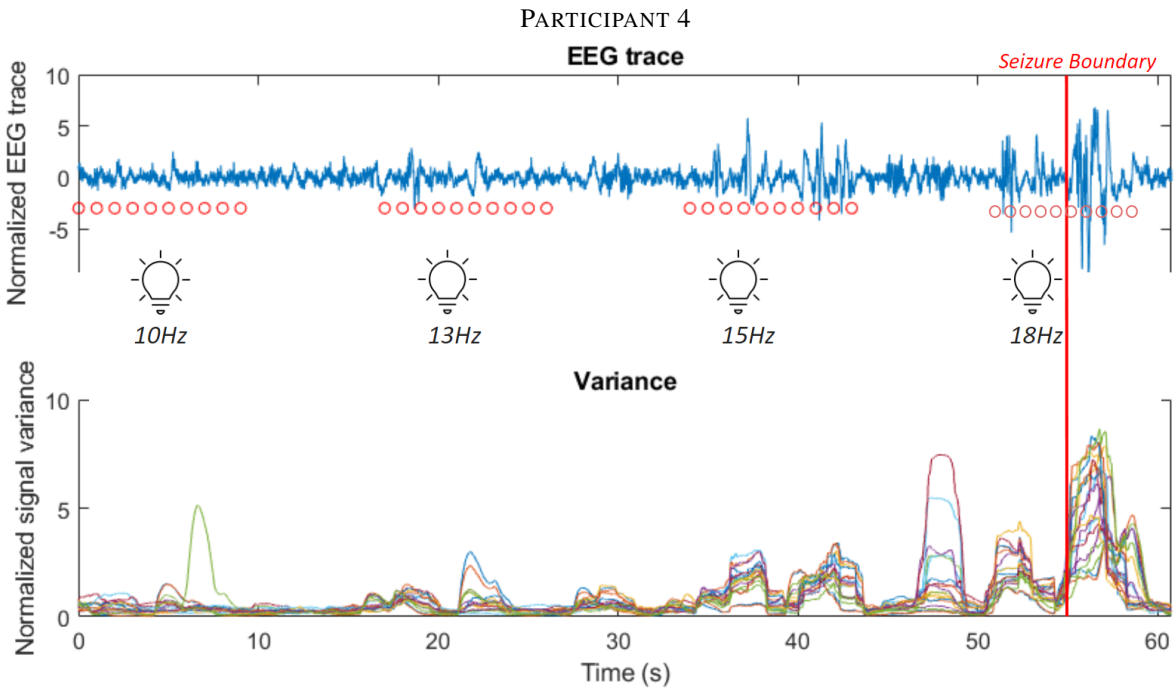

Figure 4: The first subplot shows the EEG trace (blue line) of participant 4 in the leadup to a PPR, visible as high amplitude spiking activity after the marked seizure boundary (vertical red line). Consecutive red dots mark 10 seconds of photic stimulation for the frequency (labelled below them). Below, the corresponding variance of the signal is displayed, using the shared time axis (y-axis), where different electrode channels are displayed as different coloured lines. Observe the increasing variance close to the PPR boundary. See Supp. Fig. S1 for further participant examples.

These examples suggest that time-series measures may track changes in cortical excitability close to a state transition. However, further individual analysis would not be meaningful as there is not enough trials to analyse. The dataset only contained single trials, and multiple trials of repeated stimulation frequencies are necessary to determine the individualised, frequency-dependent response. This will be addressed in future work. Instead, to demonstrate that these measures may track cortical excitability we investigate the effect of photic stimulation as a perturbation to brain state using group-wise comparisons.

To do this, we compared the distributions of variance and autocorrelation function widths (ACFW) during photic stimulation epochs between groups. Values were pooled over all 19 electrode channels and the 10 participants in each of the four groups. We compared the cumulative distribution functions of these measures to resting controls, and observed a greater relative proportion of high values in all groups during photic stimulation (see Figure S2). This was particularly apparent in the GGE (PPR) group just prior to their first PPR ('pre-PPR'), where cortical excitability was hypothesised to be greatest.

GROUP DISTRIBUTIONS OF VARIANCE AND AUTOCORRELATION FUNCTION WIDTH (ACFW)

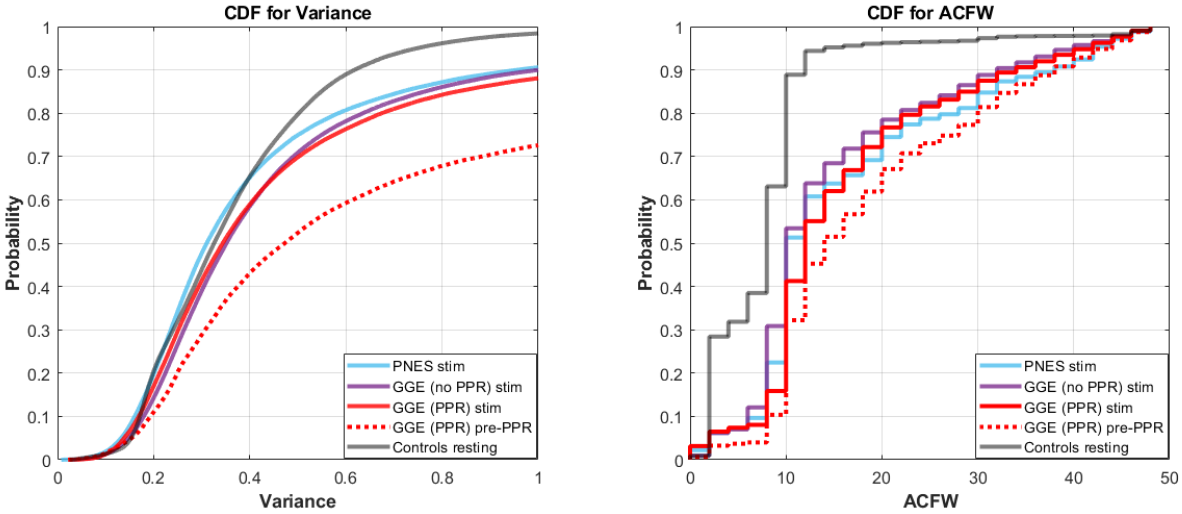

Figure 5: Cumulative distribution functions (CDF) for variance (left plots) and autocorrelation function width (ACFW; right plots), where the x-axis is the values for each measure, and the y-axis is the probability of observing a corresponding x-value and all values less than it. Each coloured line represents a different group's distribution, pooled over all participants and channels for selected epochs (refer to legend). Right-shifted lines indicate distributions with larger proportions of high values. Observe how all groups show right-shifts compared to the control (grey) line. Also observe how, for the GGE (red) group, their distributions shift further to the right, in the epoch just before PPR (dotted line labelled as 'pre-PPR'), compared to earlier stimulation epochs (solid line labeleld as 'GGE (PPR) stim').

3.3.2 Synchrony

Relative Phase

To investigate whether changes in synchrony may indicate increased cortical excitability, we constructed phase diagrams of relative phase values in stimulation epochs leading to a PPR. In some cases, we observed greater clustering in epochs close to a PPR, indicating that a particular channel pair was becoming more synchronous (marked also by longer mean vector lengths - see Fig. 6). However, clustering magnitudes varied considerably between individuals and depending on combinations of factors like channel pair, frequency band, and time to PPR, suggesting considerable individual variation. Magnitudes tended to correlate positively between frequency bands, though lower frequency bands (delta, theta, alpha) tended to have ranges extending to higher values, compared to beta and gamma which tended to have lower values overall, likely related to different degrees of freedom from bandwidth ranges S4).

To investigate whether certain channels may demonstrate greater change in synchrony, a factor analysis was performed on relative phase values during stimulation from the GGE (PPR) participants. The three dominant component factors, separated a subset of posterior channels, which demonstrated the greatest variance along these factor axes (see Fig. 7). This result was relatively consistent over all frequency bands (see Supp. Fig. S3).

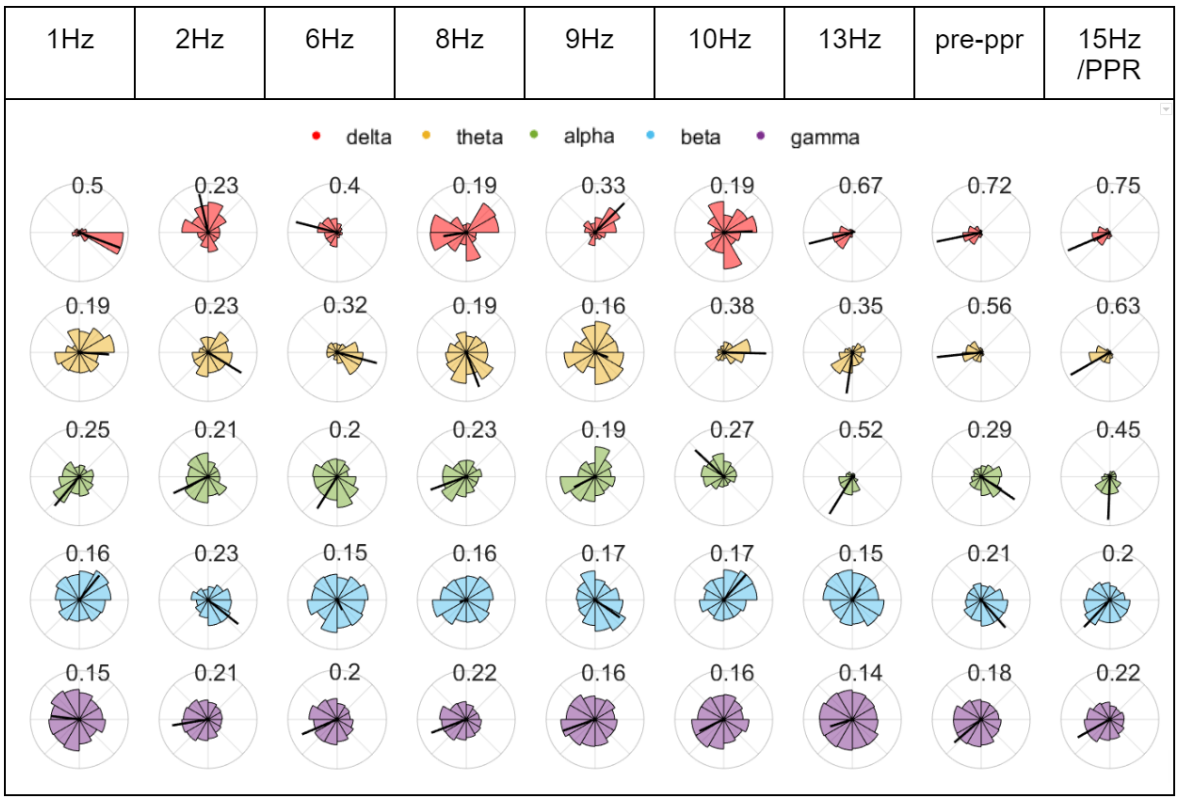

Figure 6: Chronological phase histograms during P1's stimulation train. Each plot represents 10s of binned relative phase difference values between O1 and Fz for epochs leading to the first PPR. Each bin has a direction from 0 to 2pi around the unit circle, and a length indicating the relative frequency of values, ranging from 0 to 1. The radius of each circle plot varies to assist visualisation, and the the mean relative phase amplitude (time-varying synchrony) is indicated by a black line whose length is labelled above each plot and also ranges from 0 to 1, where 1 indicates greater clustering of the values in the plot. Each row corresponds to relative phase values within different frequency bands (see legend).

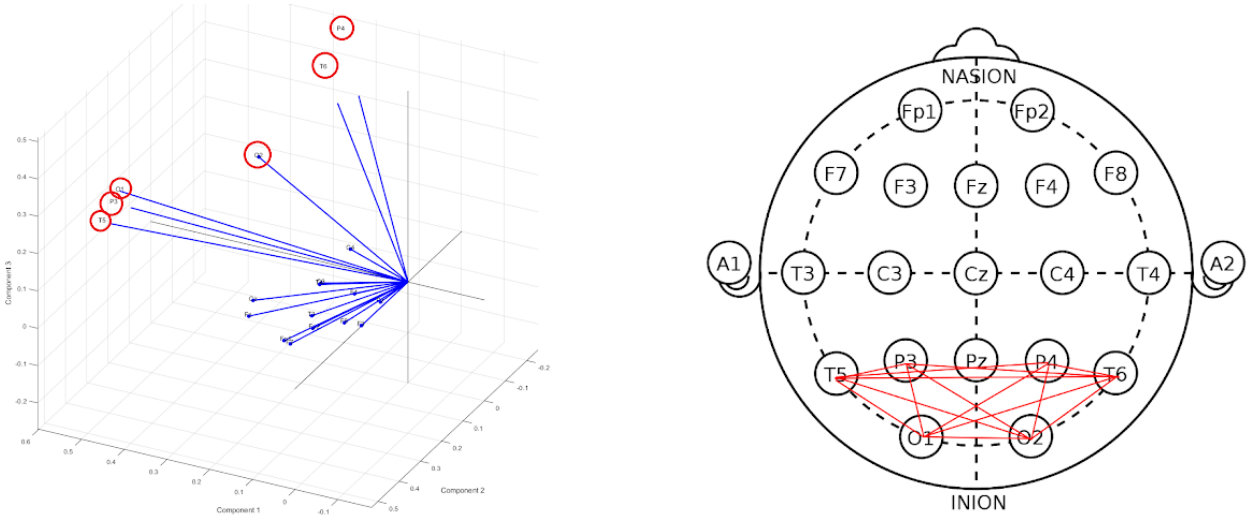

Figure 7: (A) Biplot of factor loadings (blue vectors) on the dominant component factors (axes), generated from a factor analysis of cosine of the relative phase values during photic stimulation, pooled over GGE (PPR) participants. Channels with the highest loadings, suggesting they demonstrated the greatest variance, along the component axes are P4, T6, O2, O1, P3, T5 (circled in red). Similar results were obtained when repeated in other frequency bands (see Supp. Fig. S3). (B) Subgraph of posterior channels.

Magnitude of the average phase vector

To investigate changes in synchrony in broader brain regions, we compared global and posterior synchrony in groups during photic stimulation compared to controls. Significant differences in empirical cumulative distribution functions (CDF) was found compared to controls in some frequency bands and groups (see Fig. 8 for an illustration of the CDFs, and Table 3 for a breakdown of statistical test outputs). This was most clear in the gamma band, where all groups showed a clear (and significant) difference in their distributions compared to controls, with a reduced probability of high coherence values (see Fig. 8 row 1, column 5). Marked differences in posterior synchrony distributions in all groups compared to controls is also evident in the CDF diagrams, which were found to be significant for every group in all frequency bands, except the GGE (PPR) stimulation and pre-PPR gamma distributions.

Distinction between each group photic stimulation distribution is not clear from inspection of CDF distributions, though the presence of differences relative to controls across all groups suggests a general effect of the photic stimulation on relative global and posterior synchrony, that is not specific to a particular group.

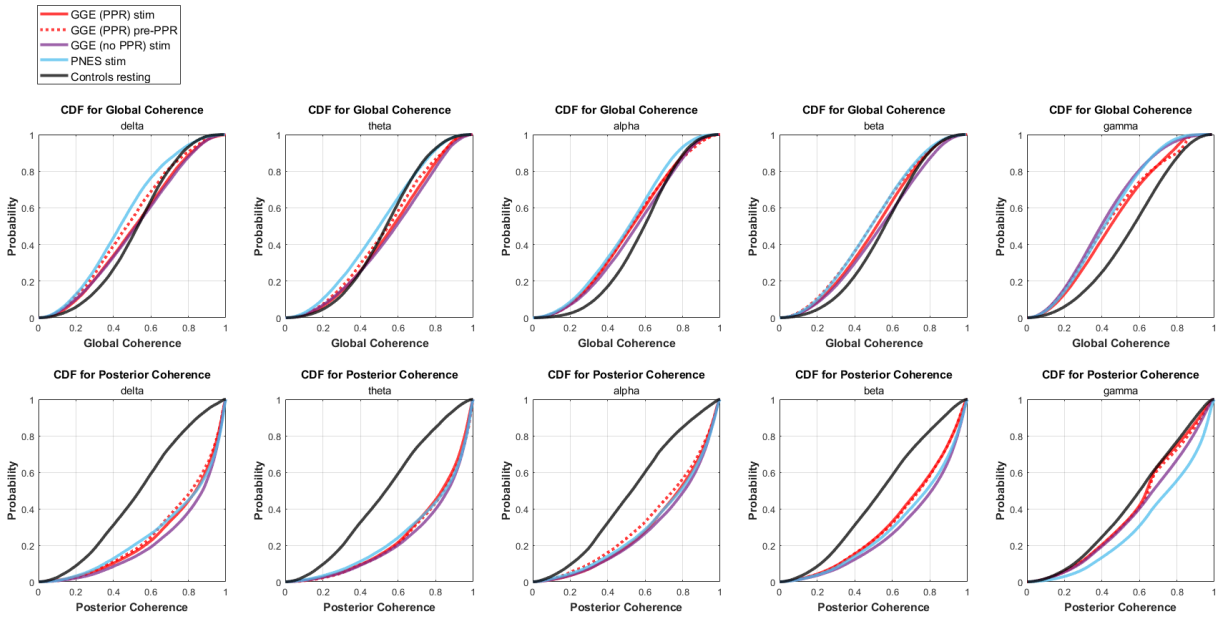

Figure 8: Empirical cumulative distribution functions (CDF) for coherence in different groups (different coloured lines, see legend), within different frequency bands (rows). The x-axis is coherence calculated as the mean phase vector magnitude over all channels (subplots in first row), or posterior (P3, P4, T5, T6, O1, O2) channels only (subplots in second row). The y-axis is the cumulative probability for the corresponding x-values. From visual inspection, there is evidence for decreased global synchrony during stimulation in the first row where left-shifts are observed compared to controls (black line), most evident in the gamma band. Increased posterior synchrony is evident in the second row in all frequency bands, with right shifted CDFs for groups during stimulation (coloured lines) compared to controls (black line). See Table 3 for a breakdown of significant differences.

Table 3: Statistical results for two-sample Kolmogorov-Smirnov tests

Frequency band	**GGE (PPR) stim**	**GGE (PPR) pre-ppr**	**GGE (no PPR) stim**	**PNES stim**
Differences between global synchrony CDFs compared to controls				
delta	$D = 0.078$	$D = 0.124$*	$D = 0.034$	$D = 0.182$*
theta	$D = 0.056$	$D = 0.038$	$D = 0.046$	$D = 0.116$
alpha	$D = 0.076$	$D = 0.070$	$D = 0.108$	$D = 0.068$
beta	$D = 0.130$*	$D = 0.132$*	$D = 0.064$	$D = 0.136$*
gamma	$D = 0.258$*	$D = 0.250$*	$D = 0.290$*	$D = 0.328$*
Differences between posterior synchrony CDFs compared to controls				
delta	$D = 0.456$*	$D = 0.368$*	$D = 0.498$*	$D = 0.396$*
theta	$D = 0.450$*	$D = 0.402$*	$D = 0.468$*	$D = 0.434$*

alpha	$D = 0.368$*	$D = 0.358$*	$D = 0.392$*	$D = 0.326$*
beta	$D = 0.292$*	$D = 0.356$*	$D = 0.412$*	$D = 0.364$*
gamma	$D = 0.116$	$D = 0.106$	$D = 0.142$*	$D = 0.242$*

* Significant with $p < 0.001$ (adjusted for multiple comparisons using bonferroni correction). D is the Kolmogorov-Smirnov test statistic.

4 Discussion

The primary finding of this study was that the response to perturbation by photic stimulation was measurable via changes in biomarkers. Specifically, the variance, autocorrelation function width (ACFW), and phase coherence distributions in all experimental groups compared to resting controls. As expected, the posterior channels demonstrated the greatest variation in synchrony. While global synchrony decreased during stimulation, posterior synchrony increased, reflecting possible underlying PPR pathophysiology mechanisms found in the literature [33; 14; 46]. Time-frequency spectra of PPR and spontaneous seizure transitions were similar, and we argue that PPR is a valid proxy for studying general seizure dynamics. Response to perturbation varied by stimulation frequency as well as individually. Greater changes were often observed in epochs closer to a PPR, though further repeated-trial analysis is necessary to establish this result.

4.1 Findings

We interpret the change in the CDFs as a data-driven illustration of theoretical stochastic predictions where an altered distribution of system statistics reflect the shifting dynamics before a state transition to seizure activity. Specifically, the changes in distribution statistics indicate an increased response to perturbation - cortical excitability - related to PPR susceptibility.

Although similar to critical slowing literature which has found increased variance and autocorrelation before seizure activity [2], we report these measures as biomarkers of the perturbation response. In the former case, changes are observed passively, while here they track actively provoked responses. Variance and autocorrelation width measures were able to separate the distribution just before PPR ('pre-PPR') from the same group's broader stimulation distribution. This suggests that they were sensitive to increased cortical excitability close to the PPR seizure boundary, making them valid biomarkers of the response to perturbation.

Motivated by previous findings that increased phase synchrony was associated with seizure-related excitability [3], we investigated changes in synchrony to evaluate if it is indeed a biomarker of cortical excitability. We observed decreased global coherence - the average coherence across all channels - across all groups compared to controls. The trend was visible in all frequency bands though only reached significance in the gamma frequency band. In comparison, when the average coherence was taken across posterior channels only, we observed increased posterior coherence compared to controls across all groups and almost all frequency bands. This is generally consistent with the literature, in which most studies report little or no change to synchrony measures [9], except in occipital electrodes where it may be seen to increase. More specifically, studies have found enhanced clustering in higher harmonic frequencies of the photic stimulation frequency just before a PPR is elicited [47], with increased synchrony expected particularly in gamma frequencies [48]. We suggest our observation of reduced global synchrony is associated with the relative increased synchrony in posterior regions that we observed. This effect appeared general, as it was observed in all epilepsy groups compared to controls. While increased gamma synchronisation is expected as part of normal visual processing, studies have found enhanced VEP amplitudes in photosensitive individuals suggestive of pathological excitability of the occipital cortex, which may underlie PPR manifestation. This is consistent with our factor analysis that observed the greatest phase clustering in the posterior electrodes. Indeed, recent reviews [47; 9] have argued that PPR likely occurs due to combinations of an enhanced neural response to flicker, and in particular, subsequent aberrant propagation of posterior synchronisation due to aberrant gain control of this high frequency neural activity.

While our results affirmed theories that photic stimulation provokes increased high frequency activity in posterior regions, it is unclear whether synchrony measures relate to cortical excitability directly. Our phase clustering measures were not sensitive enough to distinguish the pre-PPR epoch from earlier epochs in the photosensitive group, as was hypothesised. Specifically, their distributions were not separable (fig 8. Therefore, coherence may more specifically indicate the underlying PPR generating mechanism, rather than cortical excitability. Though, given the great degree of individual variation we observed, as well as variation in different stimulation epochs, we believe differences may be more evident in individualised frequency-dependent analyses (see 6 for an example). Thus, further study is needed to investigate whether synchrony measures are valid biomarkers of cortical excitability.

4.2 Limitations

In this retrospective study, there were several limitations. Because we did not have appropriate resting state recordings, we compared data to resting controls. However, ideally, each individual would be compared to their own resting or baseline distribution, to ascertain the true change from perturbation. Another issue was the considerable within-group variability we observed, undermining the validity and generalisability of the group analyses. Though, it is likely that the population distribution for each epilepsy group is itself heterogeneous, and distributions would overlap each other considerably. In fact, the response to perturbation is patient-specific, therefore we recommend that future research perform individualised analyses with multiple trials. In addition, we observed frequency-dependent differences in the response to perturbation, consistent with previous research that generally finds marked responses in the 10-20Hz range [32], and in harmonic frequencies of the PPR-evoking frequency [47]. However, it would not have been appropriate to perform a group-based frequency-dependent analysis, because of confounders like ordering effects due to variation in stimulation frequency order, possible refractory effects from PPR events, and individualised responses to perturbation.

4.3 Suggested amendments to photic stimulation protocol

Performing photic stimulation has been commonplace during routine diagnostic EEG for neurological conditions since the mid-1900s [49]. Its purpose is to diagnose patients with photosensitive epilepsy if a PPR is observed, or to rule it out when no PPR is observed [32]. Together with other evidence, it may contribute to a patient's epilepsy diagnosis. It is also sometimes used to indicate change in condition and treatment efficacy, by comparing changes in response. Further, the photosensitive frequency range is of interest as it can indicate whether lifestyle and behavioural changes can be recommended, such as avoiding media that commonly involves flashing within that frequency range, or the use of blue-lens goggles/glasses to alleviate photic sensitivity [32].

Given that PPR presence and the photosensitive range are of such clinical relevance, we recommend adjustments to the protocol. Our results indicate that standard procedures may not be sufficient for determining photosensitivity, or reliable enough to determine the photosensitive range. For example, we observed no PPR after the same stimulation frequency, which had previously induced a PPR only seconds or minutes earlier, in multiple participants, perhaps due to some refractory effect of previous PPR events. It is not understood whether a PPR itself may result in a refractory period that decreases the likelihood of observing a PPR during subsequent stimulations. Also, this within-person variability suggests that lack of PPR is not necessarily sufficient for ruling out photosensitivity. Refractory periods have been suggested for broad categories of seizures, however it is not well understood how long they last and whether they depend on the length or type of seizure. Since we argue that a PPR is a proxy seizure event, we believe it is important to leave a generous amount of time after a PPR is observed before continuing with the procedure, to account for possible refractory effects, in future studies.

In addition, we observed increased markers of excitability outside of participants' designated frequency range. This may suggest that previous stimulations may have elicited a PPR if they were repeated a number of times, or that a subsequent stimulation at a higher frequency only elicited a PPR because the previous stimulation had perturbed the patient's brain into a more excitable state. If the goal of the procedure is to determine whether photic stimulation of a particular frequency would reliably elicit a PPR, we suggest investigating the appropriate rest time between stimulations that allows brain dynamics to return to baseline.

4.4 Future Directions

Since it is likely that the response to perturbation is frequency-specific, future analyses would ideally perform repetitions of stimulation frequencies, over multiple successive sessions, to obtain results over time. This would allow the construction of robust, individualised profiles of frequency-dependent responses to perturbations. These profiles would be clinically significant in that changes to the initial measurements could be used to evaluate the efficacy of medications, which are understood to alter cortical excitability as their mode of action [50]. They could also be used to evaluate the safety of medication withdrawal by indicating whether drug removal has shifted patients to regimes of higher cortical excitability and therefore seizure risk [3; 51], and monitor disease course in the long-term.

Also, it should be noted that observing measurable responses to perturbation from photic stimulation is not limited to photosensitive individuals. We observed responses to perturbation in all groups, regardless of epilepsy diagnosis (GGE or PNES), syndrome, seizure type, age, gender, or ASM. We conclude that the response to perturbation may be observable in the general epilepsy population, suggesting that the photic stimulation paradigm offers a great potential framework for studying seizure dynamics at large. Though, with our limited cohort, we could not investigate the effect of these variables more robustly, and we encourage future research to investigate other populations with epilepsy, and whether response to perturbation may change depending on the clinical characteristics aforementioned.

Photic stimulation has the potential to overtake other methods of studying seizure dynamics, given appropriate administration. Our results suggest that the PPR transition may be a valid proxy for a seizure transition. The change in frequency spectra morphology at their transition boundaries were remarkably similar, and the observed changes to excitability measures were consistent with those observed before seizure transitions. Therefore, we argue that photic stimulation is appropriate for studying seizure dynamics in general. Also, compared to other methods of studying seizure dynamics, such as seizure provocation via medication withdrawal and sleep deprivation during hospitalisation, photic stimulation is a much safer method for studying the transition to seizure. The control over stimulation frequency and timing provide an appropriate well-controlled experimental paradigm, and medication withdrawal is not necessary - in fact, 6/10 individuals in the GGE (PPR) group were taking ASMs and still displayed PPRs.

We wish to emphasise the potential for photic stimulation to be used as a perturbation paradigm for studying general brain dynamics. Already, studies have shown how greater responses to perturbation demonstrate elevated cortical excitability associated with seizure risk in focal epilepsy [2] and cohorts of patients undergoing pre-surgical evaluations [21; 19] or with severe treatment-resistant epilepsy [20; 23]. Photic stimulation also enacts a perturbation that alters brain dynamics, measurable via the EEG. However, unlike stimulation from implants, photic stimulation is a much more accessible, non-invasive perturbation framework that could potentially be used at home - only requiring an EEG headset, appropriate software, and a monitor for administering the photic stimulation. Changes to an individual's baseline at any frequency could indicate meaningful differences to cortical excitabiliy and seizure risk, regardless of epilepsy syndrome. Also, as the response to photic stimulation differs in other diseases including migraine [31], schizophrenia [52], alzheimer's disease and mild cognitive impairment [53; 9], it's relevance as a research paradigm to studying wider diseases of brain structure or function is significant. Further, photic stimulation could be used to observe changes in cortical excitability in healthy individuals under initiating factors [32; 9] like alcohol withdrawal and sleep deprivation, to provide further insight to brain dynamics in humans.

4.5 Conclusion

During photic stimulation, we observed measurable changes in the EEG of epilepsy patients with genetic generalised epilepsy (GGE) who are photosensitive as well as who are not photosensitive, and individuals with psychogenic non-epileptic seizures (PNES), compared to controls. At a group level, photosensitive individuals demonstrated further increases just before PPR, indicating a heightened state of cortical excitability. We found the greatest variation in synchrony measures in a posterior sub-group via a factor analysis. Further, we observed decreased global coherence with increased posterior coherence, that may relate to the underlying pathophysiology of the photo-paroxysmal response. In conclusion, measures of EEG timeseries like variance and autocorrelation function width during active perturbation can indicate changes in cortical excitability as biomarkers of the perturbation response. We encourage future research to investigate the frequency-dependent, individualised response to perturbation, using an extended photic stimulation paradigm that includes repetition of stimulation frequencies.Photic stimulation has potential clinical significance in evaluating medication efficacy, disease prognosis, and as indicator of seizure risk. Further, we re-frame it as a human perturbation paradigm for studying brain dynamics.

References

[1] Marten Scheffer, Jordi Bascompte, William A Brock, Victor Brovkin, Stephen R Carpenter, Vasilis Dakos, Hermann Held, Egbert H Van Nes, Max Rietkerk, and George Sugihara. Early-warning signals for critical transitions. *Nature*, 461(7260):53–59, 2009.

[2] Matias I Maturana, Christian Meisel, Katrina Dell, Philippa J Karoly, Wendyl D'Souza, David B Grayden, Anthony N Burkitt, Premysl Jiruska, Jan Kudlacek, Jaroslav Hlinka, et al. Critical slowing down as a biomarker for seizure susceptibility. *Nature communications*, 11(1):1–12, 2020.

[3] Christian Meisel, Andreas Schulze-Bonhage, Dean Freestone, Mark James Cook, Peter Achermann, and Dietmar Plenz. Intrinsic excitability measures track antiepileptic drug action and uncover increasing/decreasing excitability over the wake/sleep cycle. *Proceedings of the National Academy of Sciences*, 112(47):14694–14699, 2015.

[4] Wei-Chih Chang, Jan Kudlacek, Jaroslav Hlinka, Jan Chvojka, Michal Hadrava, Vojtech Kumpost, Andrew D Powell, Radek Janca, Matias I Maturana, Philippa J Karoly, et al. Loss of neuronal network resilience precedes seizures and determines the ictogenic nature of interictal synaptic perturbations. *Nature neuroscience*, 21(12): 1742–1752, 2018.

[5] S Kalitzin, D Velis, P Suffczynski, J Parra, and F Lopes Da Silva. Electrical brain-stimulation paradigm for estimating the seizure onset site and the time to ictal transition in temporal lobe epilepsy. *Clinical neurophysiology*, 116(3):718–728, 2005.

[6] Paolo Manganotti, Emanuela Formaggio, Alessandra Del Felice, Silvia F Storti, Alessandro Zamboni, Alessandra Bertoldo, Antonio Fiaschi, and Gianna M Toffolo. Time-frequency analysis of short-lasting modulation of eeg induced by tms during wake, sleep deprivation and sleep. *Frontiers in human neuroscience*, 7:767, 2013.

[7] Ruben Perellón-Alfonso, María Redondo-Camós, Kilian Abellaneda-Pérez, Gabriele Cattaneo, Selma Delgado-Gallén, Goretti España-Irla, Javier Solana Sánchez, José María Tormos, Alvaro Pascual-Leone, and David Bartrés-Faz. Tms-evoked prefrontal perturbation as a toy model of brain resilience to stress during the covid-19 pandemic. *Research Square*, 2021.

[8] Didi Lamers, Silvia Landi, Roberta Mezzena, Laura Baroncelli, Vinoshene Pillai, Federica Cruciani, Sara Migliarini, Sara Mazzoleni, Massimo Pasqualetti, Maria Passafaro, et al. Perturbation of cortical excitability in a conditional model of pcdh19 disorder. *Cells*, 11(12):1939, 2022.

[9] Robert S Fisher, Jayant N Acharya, Fiona Mitchell Baumer, Jacqueline A French, Pasquale Parisi, Jessica H Solodar, Jerzy P Szaflarski, Liu Lin Thio, Benjamin Tolchin, Arnold J Wilkins, et al. Visually sensitive seizures: An updated review by the epilepsy foundation. *Epilepsia*, 63(4):739–768, 2022.

[10] George Sugihara, Robert May, Hao Ye, Chih-hao Hsieh, Ethan Deyle, Michael Fogarty, and Stephan Munch. Detecting causality in complex ecosystems. *science*, 338(6106):496–500, 2012.

[11] Ole Peters and J David Neelin. Critical phenomena in atmospheric precipitation. *Nature physics*, 2(6):393–396, 2006.

[12] Thomas Lux and Michele Marchesi. Scaling and criticality in a stochastic multi-agent model of a financial market. *Nature*, 397(6719):498–500, 1999.

[13] Fernando Lopes Da Silva, Wouter Blanes, Stiliyan N Kalitzin, Jaime Parra, Piotr Suffczynski, and Demetrios N Velis. Epilepsies as dynamical diseases of brain systems: basic models of the transition between normal and epileptic activity. *Epilepsia*, 44:72–83, 2003.

[14] Fernando H Lopes da Silva and Graham FA Harding. Transition to seizure in photosensitive epilepsy. *Epilepsy research*, 97(3):278–282, 2011.

[15] Stiliyan Kalitzin, Jaime Parra, Demetrios N Velis, and FH Lopes Da Silva. Enhancement of phase clustering in the eeg/meg gamma frequency band anticipates transitions to paroxysmal epileptiform activity in epileptic patients with known visual sensitivity. *IEEE Transactions on Biomedical Engineering*, 49(11):1279–1286, 2002.

[16] Kirsten M Fiest, Khara M Sauro, Samuel Wiebe, Scott B Patten, Churl-Su Kwon, Jonathan Dykeman, Tamara Pringsheim, Diane L Lorenzetti, and Nathalie Jetté. Prevalence and incidence of epilepsy: a systematic review and meta-analysis of international studies. *Neurology*, 88(3):296–303, 2017.

[17] Mark A Kramer, Wilson Truccolo, Uri T Eden, Kyle Q Lepage, Leigh R Hochberg, Emad N Eskandar, Joseph R Madsen, Jong W Lee, Atul Maheshwari, Eric Halgren, et al. Human seizures self-terminate across spatial scales via a critical transition. *Proceedings of the National Academy of Sciences*, 109(51):21116–21121, 2012.

[18] Viktor K Jirsa, William C Stacey, Pascale P Quilichini, Anton I Ivanov, and Christophe Bernard. On the nature of seizure dynamics. *Brain*, 137(8):2210–2230, 2014.

[19] Dean R Freestone, Levin Kuhlmann, David B Grayden, Anthony N Burkitt, Alan Lai, Timothy S Nelson, Simon Vogrin, Michael Murphy, Wendyl D'Souza, Radwa Badawy, et al. Electrical probing of cortical excitability in patients with epilepsy. *Epilepsy & Behavior*, 22:S110–S118, 2011.

[20] Mark J Cook, Terence J O'Brien, Samuel F Berkovic, Michael Murphy, Andrew Morokoff, Gavin Fabinyi, Wendyl D'Souza, Raju Yerra, John Archer, Lucas Litewka, et al. Prediction of seizure likelihood with a long-term, implanted seizure advisory system in patients with drug-resistant epilepsy: a first-in-man study. *The Lancet Neurology*, 12(6):563–571, 2013.

[21] Gregory K Bergey, Martha J Morrell, Eli M Mizrahi, Alica Goldman, David King-Stephens, Dileep Nair, Shraddha Srinivasan, Barbara Jobst, Robert E Gross, Donald C Shields, et al. Long-term treatment with responsive brain stimulation in adults with refractory partial seizures. *Neurology*, 84(8):810–817, 2015.

[22] F Wendling, U Gerber, D Cosandier-Rimele, A Nica, J De Montigny, O Raineteau, S Kalitzin, F Lopes da Silva, and P Benquet. Brain (hyper) excitability revealed by optimal electrical stimulation of gabaergic interneurons. *Brain Stimulation*, 9(6):919–932, 2016.

[23] Carolina Cuello Oderiz, Nicolás von Ellenrieder, François Dubeau, Ariella Eisenberg, Jean Gotman, Jeffery Hall, Ana-Sofía Hincapié, Dominique Hoffmann, Anne-Sophie Job, Hui Ming Khoo, et al. Association of cortical stimulation–induced seizure with surgical outcome in patients with focal drug-resistant epilepsy. *JAMA neurology*, 76(9):1070–1078, 2019.

[24] Recep A Ozdemir, Ehsan Tadayon, Pierre Boucher, Haoqi Sun, Davide Momi, Wolfgang Ganglberger, M Brandon Westover, Alvaro Pascual-Leone, Emiliano Santarnecchi, and Mouhsin M Shafi. Cortical responses to noninvasive perturbations enable individual brain fingerprinting. *Brain stimulation*, 14(2):391–403, 2021.

[25] GFA Harding, CE Herrick, and PM Jeavons. A controlled study of the effect of sodium valproate on photosensitive epilepsy and its prognosis. *Epilepsia*, 19(6):555–565, 1978.

[26] CD Binnie, DGA Kasteleijn-Nolst Trenité, and R De Korte. Photosensitivity as a model for acute antiepileptic drug studies. *Electroencephalography and clinical neurophysiology*, 63(1):35–41, 1986.

[27] Jacqueline A French, Gregory L Krauss, Dorothee Kasteleijn, Bree D DiVentura, and Emilia Bagiella. Effects of marketed antiepileptic drugs and placebo in the human photosensitivity screening protocol. *Neurotherapeutics*, 11:412–418, 2014.

[28] Jacqueline A French, Robert Wechsler, Michael A Gelfand, John R Pollard, Blanca Vazquez, Daniel Friedman, Lily H Gong, Edwin Kamemoto, Jouko Isojarvi, and James V Cassella. Inhaled alprazolam rapidly suppresses epileptic activity in photosensitive participants. *Epilepsia*, 60(8):1602–1609, 2019.

[29] Dorothee GA Kasteleijn-Nolst Trenite, Bree D DiVentura, John R Pollard, Gregory L Krauss, Sarah Mizne, and Jacqueline A French. Suppression of the photoparoxysmal response in photosensitive epilepsy with cenobamate (ykp3089). *Neurology*, 93(6):e559–e567, 2019.

[30] Gianluca Coppola, Cherubino Di Lorenzo, Vincenzo Parisi, Marco Lisicki, Mariano Serrao, and Francesco Pierelli. Clinical neurophysiology of migraine with aura. *The journal of headache and pain*, 20(1):1–10, 2019.

[31] Marina De Tommaso, Sebastiano Stramaglia, Daniele Marinazzo, Gabriele Trotta, and Mario Pellicoro. Functional and effective connectivity in eeg alpha and beta bands during intermittent flash stimulation in migraine with and without aura. *Cephalalgia*, 33(11):938–947, 2013.

[32] Dorothée Kasteleijn-Nolst Trenité, Guido Rubboli, Edouard Hirsch, Antonio Martins da Silva, Stefano Seri, Arnold Wilkins, Jaime Parra, Athanasios Covanis, Maurizio Elia, Giuseppe Capovilla, et al. Methodology of photic stimulation revisited: updated european algorithm for visual stimulation in the eeg laboratory. *Epilepsia*, 53(1):16–24, 2012.

[33] Arnold J Wilkins, Paolo Bonanni, Vittorio Porciatti, and Renzo Guerrini. Physiology of human photosensitivity. *Epilepsia*, 45:7–13, 2004.

[34] Anna Elisabetta Vaudano, Andrea Ruggieri, Pietro Avanzini, Giuliana Gessaroli, Gaetano Cantalupo, Antonietta Coppola, Sanjay M Sisodiya, and Stefano Meletti. Photosensitive epilepsy is associated with reduced inhibition of alpha rhythm generating networks. *Brain*, 140(4):981–997, 2017.

[35] Sarah M Haigh, Nicholas R Cooper, and AJ Wilkins. Chromaticity separation and the alpha response. *Neuropsychologia*, 108:1–5, 2018.

[36] Hyunho Chu, Chun Kee Chung, Woorim Jeong, and Kwang-Hyun Cho. Predicting epileptic seizures from scalp eeg based on attractor state analysis. *Computer methods and programs in biomedicine*, 143:75–87, 2017.

[37] Daniel Millman, Stefan Mihalas, Alfredo Kirkwood, and Ernst Niebur. Self-organized criticality occurs in non-conservative neuronal networks during 'up'states. *Nature physics*, 6(10):801–805, 2010.

[38] Mikhail Genkin, Owen Hughes, and Tatiana A Engel. Learning non-stationary langevin dynamics from stochastic observations of latent trajectories. *Nature Communications*, 12(1):5986, 2021.

[39] Ingrid E Scheffer, Samuel Berkovic, Giuseppe Capovilla, Mary B Connolly, Jacqueline French, Laura Guilhoto, Edouard Hirsch, Satish Jain, Gary W Mathern, Solomon L Moshé, et al. Ilae classification of the epilepsies: position paper of the ilae commission for classification and terminology. *Epilepsia*, 58(4):512–521, 2017.

[40] Udaya Seneviratne, David Reutens, and Wendyl D'Souza. Stereotypy of psychogenic nonepileptic seizures: Insights from video-eeg monitoring. *Epilepsia*, 51(7):1159–1168, 2010.

[41] Mastaneh Torkamani-Azar, Sumeyra Demir Kanik, Serap Aydin, and Mujdat Cetin. Prediction of reaction time and vigilance variability from spatio-spectral features of resting-state eeg in a long sustained attention task. *IEEE journal of biomedical and health informatics*, 24(9):2550–2558, 2020.

[42] Periklis Y Ktonas and Nicola Papp. Instantaneous envelope and phase extraction from real signals: theory, implementation, and an application to eeg analysis. *Signal Processing*, 2(4):373–385, 1980.

[43] Fredrik Gustafsson. Determining the initial states in forward-backward filtering. *IEEE Transactions on signal processing*, 44(4):988–992, 1996.

[44] Hamed Honari, Ann S Choe, and Martin A Lindquist. Evaluating phase synchronization methods in fmri: A comparison study and new approaches. *NeuroImage*, 228:117704, 2021.

[45] Robert H Riffenburgh. *Statistics in medicine*. Academic press, 2012.

[46] Gionata Strigaro, Benedetta Gori, Claudia Varrasi, Thomas Fleetwood, Giorgio Cantello, and Roberto Cantello. Flash-evoked high-frequency eeg oscillations in photosensitive epilepsies. *Epilepsy Research*, 172:106597, 2021.

[47] J Parra, SN Kalitzin, J Iriarte, W Blanes, DN Velis, and FH Lopes da Silva. Gamma-band phase clustering and photosensitivity: is there an underlying mechanism common to photosensitive epilepsy and visual perception? *Brain*, 126(5):1164–1172, 2003.

[48] Vittorio Porciatti, Paolo Bonanni, Adriana Fiorentini, and Renzo Guerrini. Lack of cortical contrast gain control in human photosensitive epilepsy. *Nature neuroscience*, 3(3):259–263, 2000.

[49] AC Mundy-Castle. The clinical significance of photic stimulation. *Electroencephalography and Clinical Neurophysiology*, 5(2):187–202, 1953.

[50] Isabella Premoli, Andrea Biondi, Sara Carlesso, Davide Rivolta, and Mark P Richardson. Lamotrigine and levetiracetam exert a similar modulation of tms-evoked eeg potentials. *Epilepsia*, 58(1):42–50, 2017.

[51] Christian Meisel, Dietmar Plenz, Andreas Schulze-Bonhage, and Heinz Reichmann. Quantifying antiepileptic drug effects using intrinsic excitability measures. *Epilepsia*, 57(11):e210–e215, 2016.

[52] Galina V Portnova and Aleksandra V Maslennikova. The photic stimulation has an impact on the reproduction of 10 s intervals only in healthy controls but not in patients with schizophrenia: The eeg study. *Brain Sciences*, 13(1): 112, 2023.

[53] Dohyun Kim, Jin-seok Park, Hojin Choi, Hokyoung Ryu, and Kyoungwon Seo. Deep learning model for early screening of patients with alzheimer's disease and mild cognitive impairment using eeg-ssvep. *HCI* , pages 781–787, 2023.